Electronics Research Laboratory
University of California
Berkeley, California
Internal Technical Memorandum M-72

LOW TEMPERATURE PLASMA EXPERIMENT FOR STUDY OF HIGH TEMPERATURE PLASMA INSTABILITIES*

by

Charles K. Birdsall**
Jack A. Byers
Tao Yuan Chang

* The research reported herein is made possible through support received from the Departments of Army, Navy, and Air Force under Contract AF-AFOSR 139-6u and the Department of Air Force, Aeronautical Systems Division under Contract AF 33(615)-1078.

** Miller Institue for Basic Research in Science, 1963-1964.

May 19, 1964

INTRODUCTION TO THE EXPERIMENT

Experiments on thermal plasmas with kilo electron volt energies and with densities like 10^{14} cm^{-3} are very difficult and very expensive in time and equipment. Experiments at lower energies and densities on steady-state plasmas can be considerably less expensive. Fortunately, there is the possibility of performing experiments on low energy plasmas which simulate some of the behavior at high energies, especially with respect to instabilities, such as growth of flutes. Because of the importance of understanding and preventing instabilities, experiments at low energies have become very attractive. The purpose of this report is to show that there is strong analogy between the high and low energy regimes using a particular set of parameters.

The low temperature plasma will use positive ions of atoms with low ionization potential, such as the alkalis (Li, Na, K, Cs) or Ba, to be obtained from surface ionization on high work function metal or insulator plates. The electrons are to be obtained from thermionic emission, generally from the same emitter used for the ions. The plasma temperature will be about that of the plates, roughly 2000^{o} K, or 0.2 eV. Thus the plasma source will consist of one or more hot plates, with the alkali atoms obtained from an oven (molecular beam mode) or from the background gas (vapor pressure mode). Such techniques are well known with extensive journal publication (see, for example, Rynn, 1964); these are not discussed here.

The plasma configurations of most interest to us at present are those in mirror fields. Thus, the experimental design and objectives are tied to mirror fields and the modification of mirror fields.

Sec. I presents some ideas on the choice of parameters for the low temperature plasma and comparison with a hot plasma. The key is to show in the ranges chosen that the collision effects do not dominate over the flute growth in mirror fields. In the model using two source plates (one at each B_{max}, "in" the mirrors) see Fig. 1, line tying, or shorting out of E in the central region, due to conduction to the end plates, can be reduced by a large resistivity $\eta_{||}$; however, this is in conflict with good communication along field lines for flute growth of long wavelength along B_o. In the new model proposed, using a central source plate, see Fig. 2, line tying is not possible for $r > r_{plate}$, so that there is no line tying problem, no conflict with large $\lambda_{||}$ flute growth; furthermore, the spatial distribution of the plasma is much improved. This idea was suggested by T. Y. Chang.

Sec. II presents briefly some of the initial experiments proposed.

I. CHOICE OF PARAMETERS: COMPARISON WITH A HOT PLASMA

The purpose of this effort is to simulate a hot plasma with a cold plasma. It is most important to make the analogy as close as possible through careful choice of parameters. The analogy in this case means the equivalence of all important characteristic quantities of the plasma when the units of mass, length, and time are scaled according to a definite set of rules. The scaling is presented in Sec. A and B, to follow. Secs. C and D discuss line tying and the central plate source. Sec. E discusses finite gyroradius stabilization effects.

A. RANGES OF n, T_i, $_e$, B, m_+ IN TERMS OF CHARACTERISTIC LENGTHS D AND r_g

In Figs. 3 and 4 the fundamental plasma quantities are plotted as functions of experimental parameters. (The constants and formulas used follow these figures.) The regions for hot, thermonuclear plasmas and cold alkali-metal plasmas are indicated on both diagrams as regions I and II, respectively (somewhat arbitrarily chosen). Region I is for

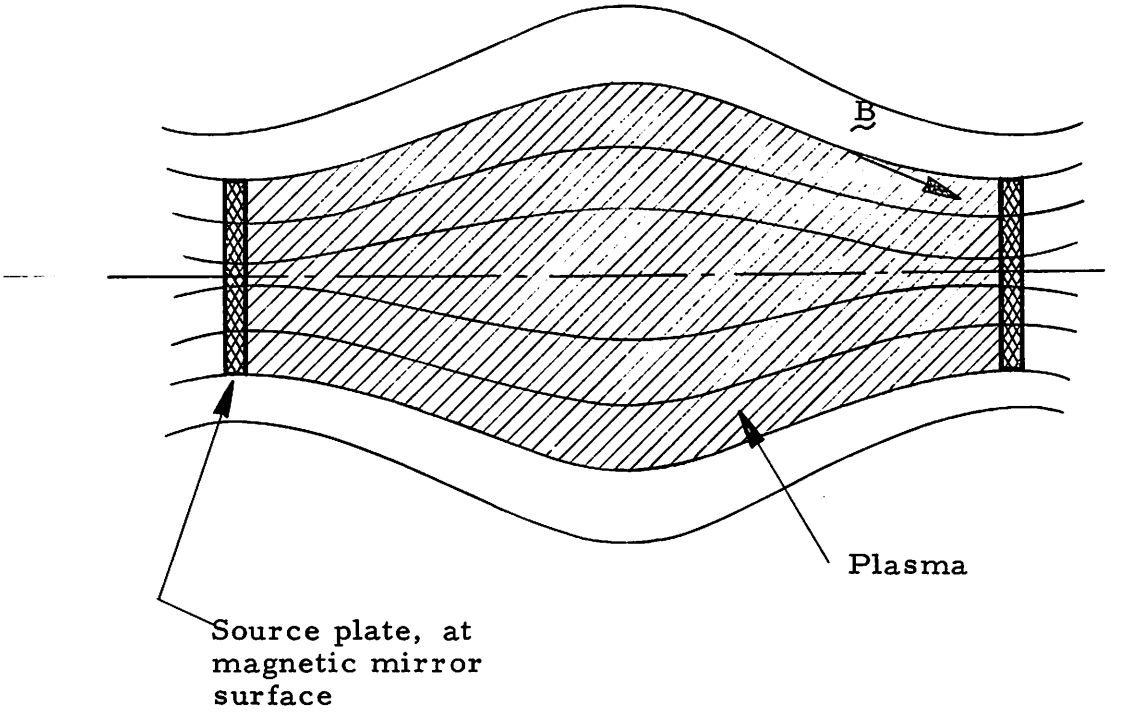

Fig. 1. Two-source plate low temperature experiment.

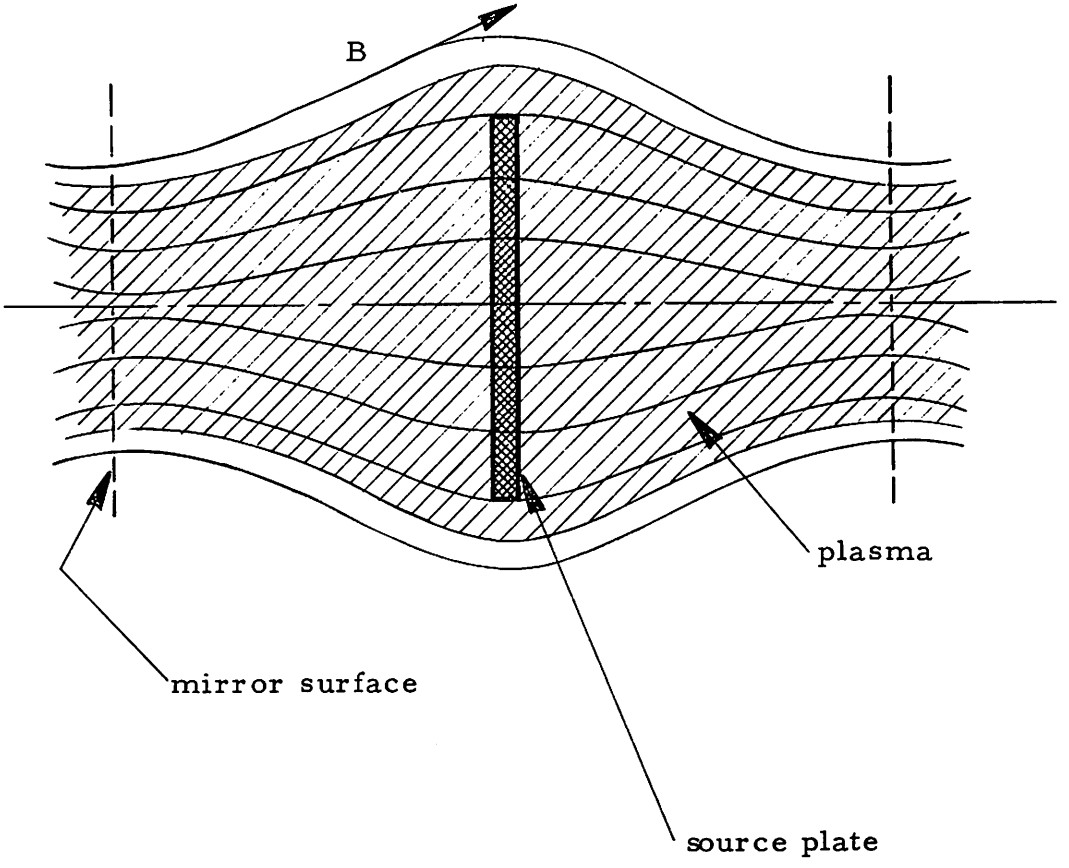

Fig. 2. Central source plate low temperature experiment.

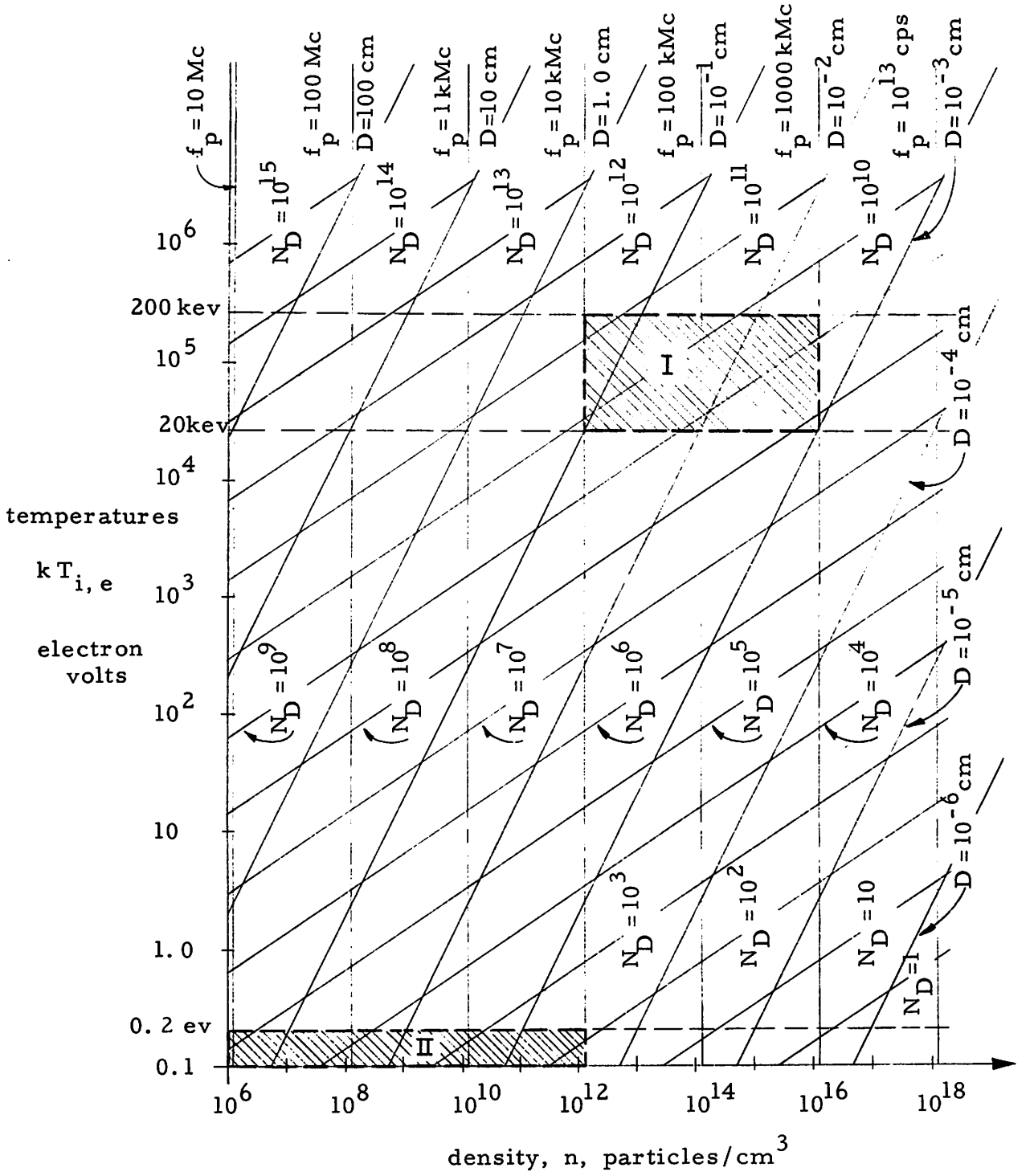

Fig. 3. Region I is a typical high temperature plasma with energies of 20 to 200 kiloelectron volts. Region II is the analogous low temperature plasma, with energies of 0.1 to 0.2 ev. D is the Debye shielding length. N_D is the number of particles in a Debye sphere. f_p is the electron plasma frequency.

N, D, and f_p as functions of density, n, and temperature, T, for typical high temperature plasmas, Region I, and typical low plasmas, Region II.

Debye length

$$D \equiv \frac{v_T}{\omega_p} = \left(\frac{kT}{4\pi ne^2}\right)^{1/2} = 6.90\left(\frac{T}{n}\right)^{1/2} = 740\sqrt{\frac{V_T}{n}} \quad \text{cm.}$$

V_T in electron-volts, using $eV_T = kT$.

Number in a Debye sphere

$$N_D \equiv n\,\frac{4}{3}\,\pi D^3 \ .$$

Plasma frequency

$$f_p \equiv \frac{\omega_p}{2\pi} \equiv \left(\frac{ne^2}{\pi m_e}\right)^{1/2} = 8.97 \times 10^3\, n^{1/2} \ .$$

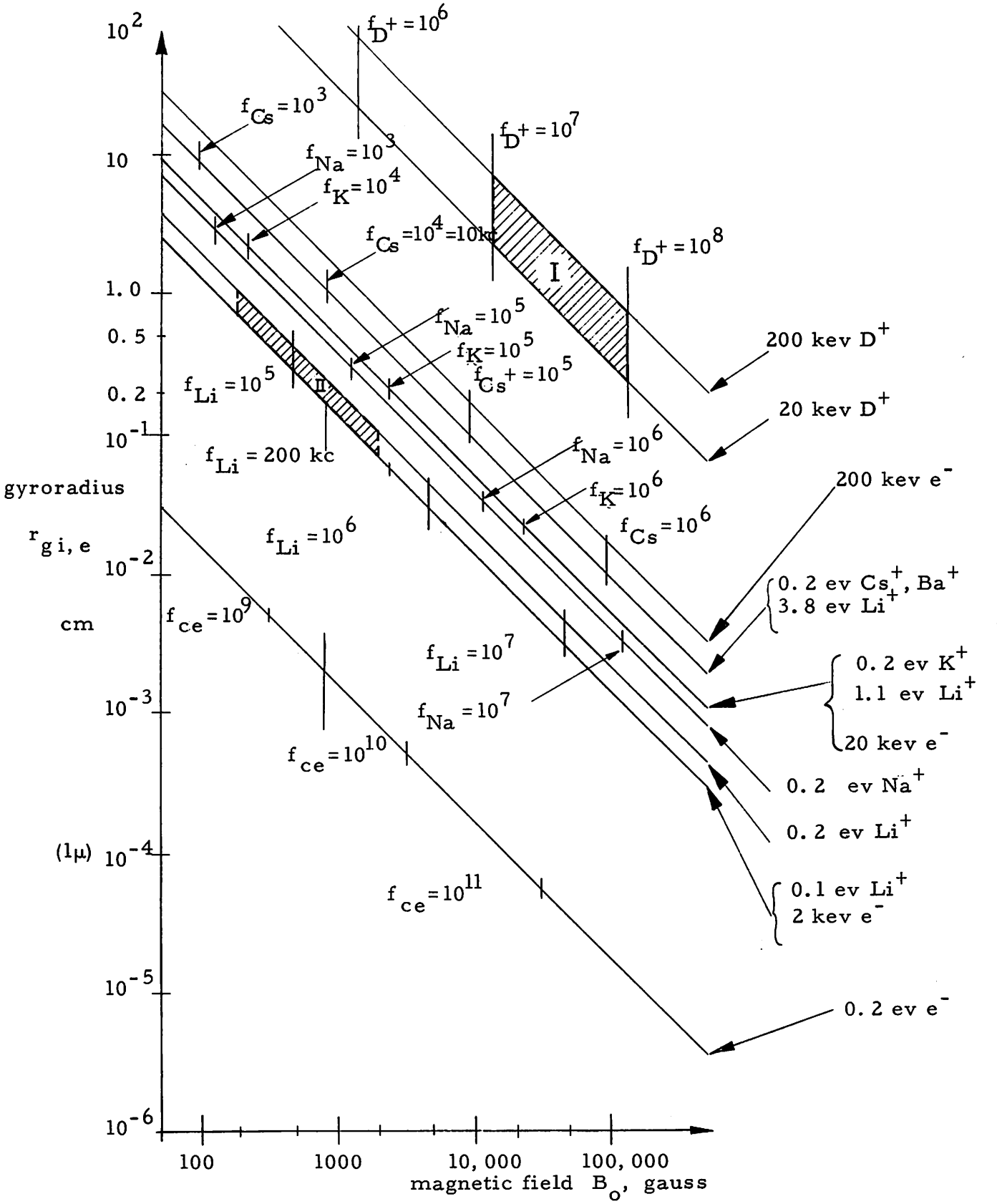

Fig. 4. Gyroradii of single electrons and ions for various temperatures and magnetic fields. Also noted are ion and electron cyclotron frequencies as a function of field.

Gyroradii as a function of magnetic field for various ions at low and high temperatures; the ion cyclotron frequencies are also noted.

Cyclotron frequency

$$f_{ce} \equiv \frac{1}{2\pi}\,\omega_{ce} \equiv \frac{1}{2\pi}\,\frac{eB_o}{m_e c} = 2.78 \text{ Mc/gauss}$$

$$f_{ci} \equiv \frac{1}{2\pi}\,\omega_{ci} \equiv \frac{1}{2\pi}\,\frac{eB_o}{m_i c} = 1.51 \text{ kc/gauss for protons}$$

Masses

m_D = 2m proton	f_{c_d} = 760 c/gauss
m_{Li} = 7m proton	$f_{c_{Le}}$ = 216 c/gauss
m_{Na} = 23 m proton	$f_{c_{Na}}$ = 64 c/gauss
m_K = 39 m proton	f_{c_K} = 39 c/gauss
m_{Rb} = 85 m proton	$f_{c_{Rb}}$ = 18 c/gauss
m_{Cs} = 133 m proton	$f_{c_{Cs}}$ = 11.3 c/gauss
m_{Ba} = 137 m proton	$f_{c_{Ba}}$ = 11 c/gauss

Gyroradius

$$r_g \equiv \frac{v_\perp}{\omega_c} \equiv \frac{\sqrt{2kT/m}}{eB_o/mc} \equiv \frac{\sqrt{2eV_T/m}}{eB_o/mc} = 3.37\,\frac{\sqrt{V_T}}{B_o} \text{ cm for electrons}$$

(V_T in ev, B_o in gauss)

$$r_{gi} = 3.37\sqrt{V_T}/B_o\ \sqrt{mi/me} \text{ cm}$$

$$r_{gLi} = 38\sqrt{V_T}/B_o \text{ cm}$$

$$r_{g_{Cs}} = 165\sqrt{V_T}/B \text{ cm}\ .$$

20 to 200 keV deuterons with densities of 10^{12} to 10^{16} cm^{-3}, in 20 to 200 kilogauss fields; region II is for 0.1 to 0.2 eV ions in 200 to 2000 gauss fields. The choice of parameters can be made conveniently with these diagrams.

B. LENGTH-TIME SCALING FOR FLUTE GROWTH, DIFFUSION VELOCITIES, COLLISION RATES

We present here the parameters of a cold lithium plasma (0.2 eV) and its comparison with a hot deuterium plasma (20 keV). From Fig. 4 we see that the cyclotron frequencies compare as $f_{D^+} \cong 300\, f_{Li^+}$. If we demand the same time scaling for plasma frequencies, then, from Fig. 3, we must choose $n_{Li} \cong 10^9$ cm^{-3}. We use this as an initial choice of n. Note that this choice gives the same Debye length, $D \cong 10^{-2}$ cm, for both plasmas; this is of minor concern as the plasma diameter in both models will generally be centimeters, many times D. Also, the number in a Debye sphere, $n\frac{4}{3}\pi D^3$, is about 10^{10} (hot plasma) as against 10^4 (cold plasma), interesting only as both should be large to qualify as a thermal plasma. On the other hand, the gyroradii, from Fig. 4, scale as $r_{D^+} \cong 4r_{Li}$, a scaling difference that will be taken into account. Note that $n_o \cong 10^9$ is a vacuum of 2×10^{-8} torr; hence $n < 10^9$ requires an excellent vacuum, making for some difficulty.

For a cesium plasma, the scaling is enough different to warrant noting. Let region II still be defined by fields of 200 to 2000 gauss. Then $f_{D^+} \cong 6000\, f_{cs}$; however, to scale f_p by this same ratio would require $n = 10^6$ cm^{-3}. As $n_o \cong 10^6$ cm^{-3} is a pressure of 2×10^{-11}, this scaling is not attractive. In order to have density like $n = 10^9$, and keep f_c and f_p time scaling, it is necessary to move region II, for C_s to 2000 to 20,000 gauss, that is, ten times the field needed for Li.

For the plasma temperature, we assign a value of 0.2 eV., or 2,320°K, which is about the maximum practical temperature for the hot plates. For the magnetic field, we use 2,000 gauss. The diameter of the plasma will be a fraction of the inner diameter of the available

coils, which is nine inches. The shape and the length of the plasma depends on the experiment and will not be assigned at the stage. However, the radius of curvature R, which is needed in the calculation of flute growth rate, is arbitrarily assumed to be 50 cm. All of the characteristic quantities of the plasma can now be calculated from these parameters using some reasonable assumptions concerning density gradients. These quantities are presented in the first column in Table I.

N_D is the number of particles in a Debye sphere, $4/3\ \pi n D^3$.

τ flute is the (e-folding) growth time of a flute (Rosenbluth and Longmire, 1957).

$$\tau_{flute} = \left[R\varkappa/\left(v_{\parallel i}^2 + 1/2\ v_{\perp i}^2\right)\right]^{1/2} = \left[\frac{m_i R\varkappa}{kT}\right]^{1/2} \text{ sec.} \qquad (1)$$

The reduced wavelength is $\varkappa$ = (plasma radius)/m; measured azimuthally, $\varkappa$ is arbitrarily assumed to be R/100, roughly an m = 5 mode on a 5 cm diameter plasma.

v_{D_η} is the classical diffusion velocity (Spitzer 1962).

$$v_{D_\eta} \equiv -D_i \frac{\nabla n}{n} \equiv -\left(\frac{nkT}{B^2}\right)\eta \frac{\nabla n}{n} = \frac{1.78 \times 10^{-3}\ Z \ln\Lambda}{B^2\ T^{1/2}} \nabla n, \text{ cm/sec.} \qquad (2)$$

∇n is arbitrarily assumed to be equal to $-(100n/R)$.

v_{D_t} is the Bohm diffusion velocity (Spitzer 1962)

$$v_{D_t} = -\frac{5.4 \times 10^2\ T}{B} \frac{\nabla n}{n} \quad \text{cm/sec} \qquad (3)$$

$\nabla n/n$ is arbitrarily assumed to be $-(100/R)$.

v_R is the curvature drift velocity (Spitzer 1962)

$$v_R = \frac{v_\parallel^2}{R\omega_c} \simeq \frac{ckT}{eBR} \quad \text{cm/sec} \qquad (4)$$

$$\left(= \frac{kT}{eBR} \quad \text{m/sec}\right)^*$$

---

*Eqs. in ( ) are in MKS units.

TABLE I. COMPARISON OF A COLD LI PLASMA WITH A HOT D PLASMA

Quantity		Cold Li Plasma	Scaling Relation L = 0.5, T = 300 sec gives first column	Hot D Plasma
mass	M_i	7 amu		2 amu
density	n	10^9 cm^{-3}		10^{14} cm^{-3}
energy	kT	0.2 eV		20 kev
field	B	2 kG		100 kG
radius of curvature	R	50 cm	100 L	100 cm
ion gyroradius	r_{ci}	0.1 cm	0.2 L	0.3 cm
electron "	r_{ce}	6×10^{-4} cm	1.2×10^{-3} L	5×10^{-3} cm
Debye length	D	10^{-2} cm	2×10^{-2} L	10^{-2} cm
0.1 R/D		500	500	1,000
D/r_{ce}		17	17	2
r_{ci}/D		10	10	30
no./Debye sphere	N_D	5×10^3	5×10^3	5×10^8
electron plasma freq.	f_{pe}	3×10^8 sec^{-1}	9×10^{10} T^{-1}	10^{11} sec^{-1}
electron cyclotron freq.	f_{ce}	6×10^9 sec^{-1}	1.8×10^{12} T^{-1}	3×10^{11} sec^{-1}
ion cyclotron freq.	f_{ci}	4×10^5 sec^{-1}	1.2×10^8 T^{-1}	8×10^7 sec^{-1}
flute growth time	τ_{flute}	3×10^{-5} sec	10^{-7} T	10^{-7} sec
resistive diffusion velocity	$v_{D\eta}$	0.2 cm/sec	1.2×10^2 L/T	2.3×10^{-2} cm/sec
Bohm diffusion velocity	v_{Dt}	10^3 cm/sec	6×10^5 L/T	10^6 cm/sec
curvature drift vel.	v_R	2×10^2 cm/sec	1.2×10^5 L/T	2×10^5 cm/sec
ion thermal vel.	v_i	2.4×10^5 cm/sec	1.4×10^8 L/T	1.4×10^8 cm/sec
Alfven vel.	v_{Alfven}	5.2×10^9	3.1×10^{12} L/T	1.6×10^9 cm/sec
dielectric constant	$K_\perp$	34	34	410
lnΛ		10.4	10.4	18
collision time	τ_{ei}	5.8×10^{-6} sec	1.9×10^{-8} T	1.1×10^{-3} sec
" "	τ_{ee}	2.8×10^{-6} sec	9.3×10^{-9} T	6.4×10^{-4} sec
" "	τ_{ii}	3.2×10^{-4} sec	1.1×10^{-6} T	3.9×10^{-2} sec
" "	τ_{in}	$\sim$ 1 sec	$\sim$ 300 T	$\sim$100 sec
relaxation time	$\epsilon_\perp/\sigma_\perp$	5.1×10^{-2}	1.7×10^{-4}	2.1 sec
time constant	$\epsilon_o\eta$	5.4×10^{-14} sec	1.8×10^{-16} T	2.9×10^{-21} sec
pressure ratio	β	2×10^{-9}	2×10^{-9}	8×10^{-13}
energy ratio	eV_e/kT	2×10^{-3}	2×10^{-3}	3×10^{-3}

v_i is the ion thermal velocity,

$K_\perp$ is the low frequency transverse dielectric constant of the plasma,

$$K_\perp = \frac{\epsilon_\perp}{\epsilon_o} = 1 + \frac{4\pi \rho_m c^2}{B^2} \cong 1 + \frac{\omega_{pi}^2}{\omega_{ci}^2} \left(= 1 + \frac{\rho_m}{\epsilon_o B^2} \right) \tag{5}$$

$K_\perp >> 1$ is required in the hydromagnetic approximation; i.e., dropping the 1 is equivalent to ignoring displacement current.

τ_{ei} is an equivalent electron-ion collision time defined by

$$\tau_{ei} = \frac{m_e c^2}{\eta n e^2} \left(= \frac{m_e}{\eta n e^2} \right) \text{ sec.} \tag{6}$$

where η is the resistivity of the plasma, (Spitzer 1962)

$$\eta = 6.53 \times 10^3 \frac{\ln \Lambda}{T^{3/2}} \quad \text{ohm-cm} \tag{7}$$

τ_{ee} is the electron self collision time.

τ_{ii} is the ion self collision time (Spitzer 1962)

$$\tau_{ii} = \frac{11.4 A^{1/2} T^{3/2}}{n Z^4 \ln \Lambda} \quad \text{sec.} \tag{8}$$

τ_{in} is the ion neutral collision time,

$$\tau_{in} = \frac{1}{v_i n_o \sigma_{in}} \quad \text{sec.} \tag{9}$$

n_o is assumed to be 10^9 cm^{-3} for both cases; $p_o \cong 2 \times 10^{-8}$ torr.

$\epsilon_\perp/\sigma_\perp$ is the transverse relaxation time of the plasma.

$\sigma_\perp$ is the transverse conductivity (Rose and Clark 1961)

$$\sigma_\perp = \frac{1}{\eta} \frac{\nu_\perp^2}{\nu_\perp^2 + \omega_{ce}^2} \quad . \tag{10}$$

For collision frequency $\nu_\perp$, we use an equivalent value defined by

$$\nu_\perp = \frac{ne^2}{m_e c^2} \eta_\perp = \left(\frac{ne^2}{m_e} \eta_\perp\right) \quad \text{sec}^{-1} \quad . \tag{11}$$

Since $\omega_{ce}^2 >> \nu_\perp^2$, $\sigma_\perp$ becomes

$$\sigma_\perp = \frac{n^2 e^2}{B^2 c^2} \eta_\perp \left(= \frac{n^2 e^2}{B^2} \eta_\perp = \frac{\omega_{pe}^4}{\omega_{ce}^2} \epsilon_o^2 \eta_\perp \right) \tag{12}$$

where (Spitzer 1962) gives

$$\eta_\perp = 1.29 \times 10^4 \frac{Z \ln\Lambda}{T^{3/2}} \quad \text{ohm-cm} \tag{13}$$

eV_e/kT is the ratio of the external potential energy to the thermal energy. V_e is defined as the potential across a distance equal to r_{ci} which produces an $(\underline{E} \times \underline{B})/B^2$ drift equalling v_R.

The second column is obtained from the first column simply by converting the unit length from 1 cm to 0.5 cm, and the unit time from 1 sec to 300 sec. The third column gives the quantities for a hot deuterium plasma with $n = 10^{14}$ cm^{-3}, kT = 20 keV, B = 100 kg and R = 100 cm.

Direct comparison of column two and column three reveals that the lithium plasma is a close analogy to the hot deuterium plasma, that is, using L = 1, T = 1 reproduces much of the third column. The main

differences between the two plasmas are that in the lithium plasma lengths are smaller by a factor of two, and time rates are slower by a factor of 300. Both of these features are of great advantage to performing experiments at low temperatures.

There are, however, several nonscaling quantities. The first one is the classical diffusion velocity $v_{D\eta}$, which is greatly enhanced (scales 10^4 too fast) in the cold plasma case. However, it is to be noted that in both cases $v_{D\eta} >> v_{Dt}$. So, if Bohm diffusion (which scales well) is present in both cases, then we can ignore the classical diffusion, at least at $n = 10^9$; raising n to 10^{12} would make $v_{Dn} > v_{Dt}$, which is not desirable, ($v_{Dn} \alpha n$, $v_{Dt} \alpha \nabla n/n$).

The second nonscaling quantity is the Alfven velocity, large by 2×10^3. Actually the phase velocity of all electromagnetic waves are too large by a factor of 600 for the cold plasma. This comes from the fact that the speed of light is the same in both cases. Note that the acoustic waves whose phase velocities are proportional to the ion thermal velocity are all scaled properly.

The third nonscaling quantity is the transverse relaxation time, down by 10^4. The hot plasma is a good dielectric for $E_\perp$; the cold plasma is more like a lossy dielectric. Hence, $E_\perp$(dc) will be shorted out after about 1/20 sec in the cold plasma. Of course using $E_\perp$(ac), $f > 50$ cps will allow field penetration.

The nonscaling of N_D is no problem; we ask only that $N_D >> 1$, as it is. The nonscaling of τ_{ei}, τ_{ee}, τ_{ii}, too small by about 10^4 is of consequence only as related to instability growth times, line tying et. al., as discussed in the sections following.

The use of $n = 10^9$ in the vapor pressure mode asks for pressure of 2×10^{-8} torr. If the molecular beam mode is used, with the beam smaller than that of the plate, $r_{beam} < r_{plate}$; then, the plasma density for $r_{beam} < r < r_{plate}$ is not zero but dependent on the pressure. Also, the plate electron emission generally will be uniform so that

in this outer region, at least at the plate, $n_e > n_i$. Thus the plasma will be blanketed by a conducting layer, quite undesirable. Because of the necessity of vacuum better than, say 2×10^{-9} torr for the beam mode, we will use the pressure mode initially.

C. LINE TYING, FLUTE GROWTH IN TWO PLATE SYSTEMS

The main instability expected in plasmas in mirror type fields is the flute instability caused by the charge-separation particle drift velocities. The flexibility of the proposed experiment with respect to density of particles, n, and ion gyro-radius r_{gi} make it ideal for studying flute growth over a wide change of these parameters. In particular, the theory of flute stabilization due to finite ion gyroradius depends on both n and r_{gi}; any experiment which can easily continuously change these parameters is inherently capable of fully testing the theory.

The flutes manifest themselves by an interchange of plasma tubes extending along the lines of magnetic force. In open-ended systems (as in actual mirror-machine devices), the lines of force are free to move (and the plasma with them) while if the lines of force end in a conducting surface which is in contact with the plasma (as in the two metal plate version of the proposed device) the plasma may be prevented from making an interchange. This effect can be explained either by an MHD theory which says that the lines of force frozen into both plasma and end conducting plates will prevent the interchange, or by a particle theory which says the conducting surface short circuits the lines of force and provides a charge drainage mechanism which can dominate over the charge being provided by the charge separation drifts. The fluid theory requires a high plasma conductivity so that the plasma remains "frozen" onto the field lines; equivalently, the particle view requires a low enough ion-electron collision frequency so that the charge can freely drain along field lines which in this model, lead to the conducting end plates.

Expected flute growth times can be much shorter than resistive diffusion times (see Table I). However, in order for the flutes to grow

in the proposed two end-plate systems, the ion-electron collisions must be frequent enough to prevent the conduction to the end from dominating the charge separation. A crude estimate can be made by comparing the growth rate of an unimpeded flute (which represents the rate of growth of the charge due to the charge separation currents) to the charge decay rate due to end conduction. Note the competing effects: for uniform flute growth over the entire length of the plasma column, the communication along B_o should be good; for avoiding the short circuit at a metal plate of sheath, the opposite should be so. Thus, the two plate system which depends on plasma parameters to avoid the short circuit is a compromise at best, allowing fluting only in the central region where the curvature of the magnetic lines of force is approximately constant.

The growth rate for a freely growing flute, based on linear theory, assuming a sharp density gradient, is exp t/τ_f, where τ_{flute} was given earlier in Eq. (1). This latter time should be short compared with the charge drainage time to the end plates. The charge decay time can be given, approximately, by an R - C time constant of an equivalent circuit composed of two lines of force separated by $\lambda/2$ and short circuited a distance ℓ (= 2R) away. Or, for the m = 1 mode, the approximate model of Fig. 5 holds, with $\tau_{RC} = R_{\|} C_{\perp}$. Thus,

$$R_{\|} \cong \eta_{\|} \frac{\ell}{W(d/m)} \tag{14}$$

$$C_{\perp} \cong \epsilon_o K_{\perp} \frac{\ell W}{(d/m)} \tag{15}$$

so
$$\tau_{RC} \cong \epsilon_o \eta_{\|} K_{\perp} \left(\frac{\ell m}{d}\right)^2 . \tag{16}$$

The result is, using $\ell = 2R_o$ (d, R_o in cm v_i in cm/sec)

$$\frac{\tau_{RC}}{\tau_f} \cong \left[\left(\frac{m}{d}\right)^5 R_o^3\right]^{1/2} 4\epsilon_{\perp} \eta_{\|} v_i . \tag{17}$$

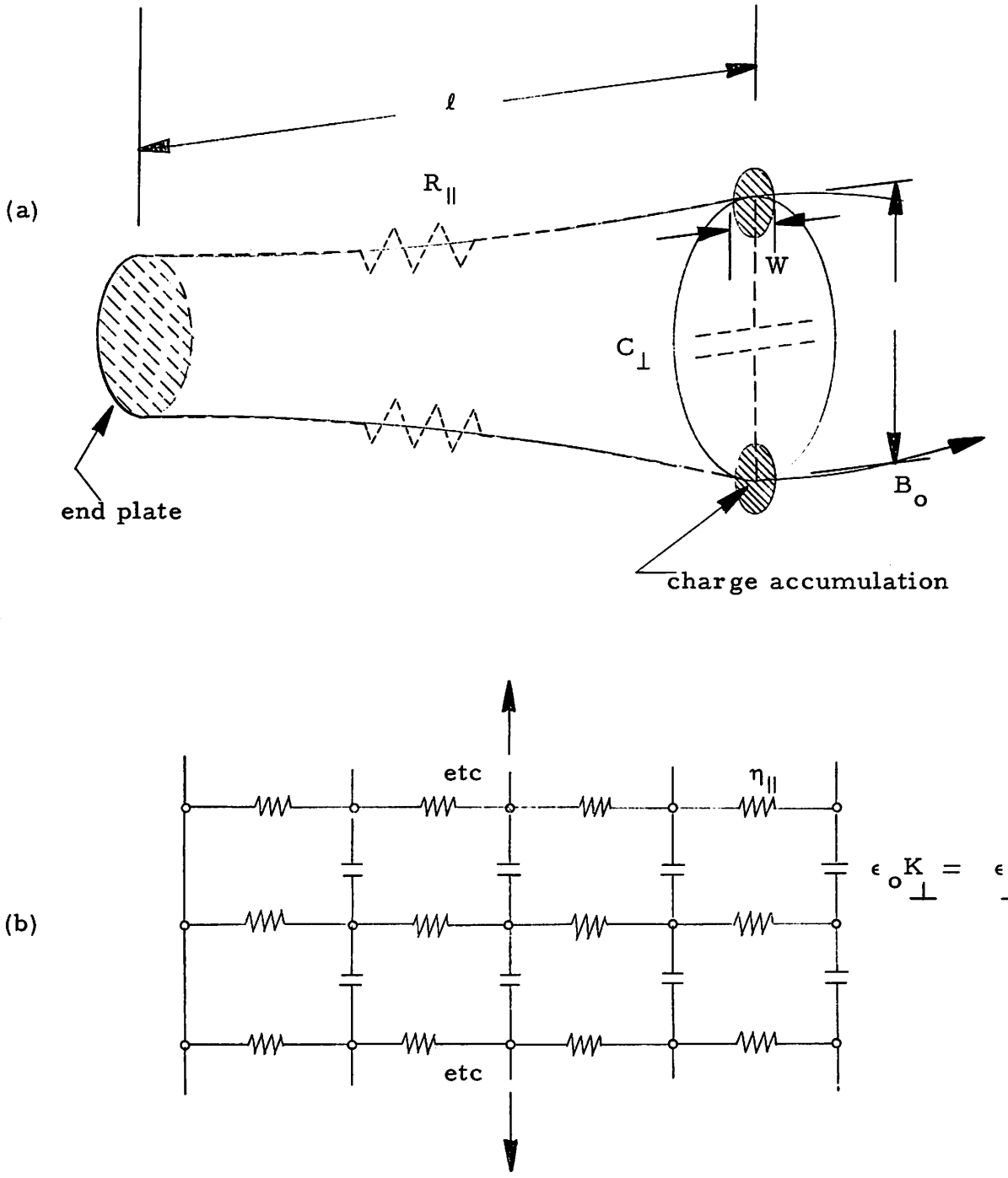

Fig. 5. (a) R-C for line tying to end plate calculation, m = 1;
(b) Equivalent network; $\sigma_{\perp}$ is neglected as it is small.

This ratio should be large for line tying to be ineffective. The values are, using Eq. (7)

$$\eta_{\parallel} = 0.62 \text{ ohm cm} \tag{18}$$

and using Eq. (5),

$$\epsilon_{\perp} = \epsilon_o K = 34\,\epsilon_o = 3 \times 10^{-12} \text{ farad/cm} \tag{19}$$

so

$$\tau_{RC} \cong 7.4 \times 10^{-12} \left(\frac{m}{d} R_o\right)^2 \quad . \tag{20}$$

This is very short unless R_o is made very large - a long skinny column; also as $\epsilon_{\perp} \sim (n\, m_i)$ is larger at higher densities, larger masses, these also increase τ_{RC}.

Finally,

$$\frac{\tau_{RC}}{\tau_f} \simeq 2.4 \times 10^{-6} \left[\left(\frac{m}{d}\right)^5 R_o^3\right]^{1/2} \quad . \tag{21}$$

For $(\tau_{RC}/\tau_f) > 1$, then $(m/d)^5 R_o^3 > 10^{11}$. Using $R = 50$ cm, then $m > 16\,d$.

Hence only the large m modes, shortest wavelengths, will be seen to grow, if at all, for the implied wavelength is less than r_{gi}. By going to Cs (increase in m_i by 19) and density of 10^{12}, (τ_{RC}/τ_f) increases by $10^3\sqrt{19}$ and the result is $m > 0.6\,d$ cm which is more attractive. Unfortunately, increasing n to 10^{12} increases the classical diffusion velocity, v_{D_η}, to twice the Bohm diffusion velocity, v_{Dt}, destroying the analogy with a collisionless plasma.

The conclusion is that line tying will be effective for $n \sim 10^9$ for a Li plasma except for absurdly large m numbers. For a Cs plasma at higher density, $n \sim 10^{12}$, $m > 3$ should be seen except that classical diffusion may wash out flute growth.

It is thus obviously desirable to find ways of obviating line tying. One such method is given in the next section. Another (thanks to S. A. Colgate) is to use insulating plates which, with high work functions like metal plates, create ion-electron pairs from neutrals; this type of source is not known to us.

An additional concern with the two plate system, is that the mirror reflection point of all particles emitted at the plates, following adiabatic motion, is at or axially beyond the plates; no particles are mirrored in the central region between plates. Thus any particles diffusing to $r > r_{plate}$ are immediately lost out the ends; it is not possible to have a sheath outside the plates which thus would not be bothered by line tying to the plates.

D. CENTRAL PLATE SOURCE

The preliminary concept of the experiment is to use a single hot disk instead of two. The hot disk is to be located at the center of the machine and supported on the axis from the ends. Ions and electrons are emitted from the disc in both directions, and are reflected back by the magnetic mirrors surfaces associated with the particle energies, not just at B_{max} as with two plates. The surface of the plasma may extend outside the hot disc without loss of all the particles as is not true for the two plate experiment; the extension is made by decreasing B_o. The plasma in the surface layer is not only trapped by the mirrors but also is detached from the hot plate. The flutes can be excited deliberately in the surface layer, and there is <u>no</u> problem of line tying to the plate. Of course, for $r < r_{plate}$, there can still be internal line tying through the $R_{\parallel} C_{\perp}$ mechanism discussed in the previous section; the stabilized central core will act as a good conductor and as

such, will maintain stability until B_o is decreased to expand the plasma. The $m = 1$ mode will be inhibited in the plate; however, using a small diameter plate will allow growth of $m = 1$ until the edge of the plasma reaches the edge of the plate.

Other benefits include reduced problems with lack of balance (potential, temperature) between two plates, and only half the heating power. This configuration is most attractive.

E. FINITE GYRORADIUS STABILIZATION EFFECTS

An extremely important consideration when calculating growth rates is the finite gyro-radius stabilization effect which must be considered whenever $(r_{gi}/\lambda)^2$ becomes comparable to $(\omega_{flute}/\omega_{ci})$ as shown by Rosenbluth, Krall, Rostoker (1961). Note that this condition can be satisfied even though $r_{gi} \ll \lambda$, i.e., this is not a scrambling effect but a charge separation due to a differential drift of ions and electrons. The differential drift is a result of the different effective E fields seen by particles of different orbit size. The difference in the effective E fields is larger for larger spatial gradients of E; the $m = 1$ mode is unaffected as the E field is constant in this mode by definition.

For our choice of parameters, the $r_{gi} \gg r_{ge}$ and r_{gi} is of appreciable size, so we should expect stabilization of modes with $m \geq 2$.

As an estimate, we use Post (1963) who gives a simplified stability criterion which applies in our case:

$$\left(\frac{L\, a_i}{r_o^2}\right) \gtrsim 1 \quad \text{stable} \quad (m \geq 2) \ .$$

Using $L = 2\ell = 100$ cm, $a_i = r_{gi} = 0.2$ cm, $r_o = d/2 = 2$ cm, we find the left hand side is 25 which easily satisfies stability.

By going to a system with smaller ℓ, larger d we could perhaps become marginally unstable for the low m modes, but it would only be marginal with decreased growth rate and very possibly the growth would then be washed out by resistive diffusion.

II. INITIAL SIMULATION EXPERIMENTS

Numerous experiments can be conceived to be performed on low energy plasmas in simulation of flute instabilities at high energies. We have chosen two experiments that are of initial interest to us. The first is study of the ordinary mirror. The second is the study of a hollow plasma in a mirror field, with possible addition of an E_r to counteract inner surface flute growth, or of B_θ (stuffing) to make a minimum B configuration. There are other things of interest, such as heating electrons or ions, but not contemplated for initial work.

A. PLASMA IN MIRROR FIELD

The initial operation will be with the simplest configuration, a cylindrical plasma in a simple mirror field. This experiment will be essentially the shakedown operation of the source, vacuum, magnet and diagnotic methods. The second step would be to look at flute stabilization with fields of varying curvature, taking advantage of the plasma (not end) line tying between regions of opposite curvature.

B. THE HOLLOW PLASMA EXPERIMENT

One type of plasma of interest to us is a hollow plasma confined in an inside-out mirror field, as in Fig. 6. The inner surface of the plasma is subject to the flute instability due to the unfavorable curvature of the magnetic field. Two possible ways are proposed to stabilize the inner surface. The first method is to pass current along the axis of the machine to form a minimum B magnetic field. The second method is to apply a centrifugal pressure on the inner surface by a radial electric field. Both variations can be investigated by an alkali-metal plasma.

Because of the short transverse relaxation time in the cold plasma, the application of a dc radial electric field will end up in a thin sheath on

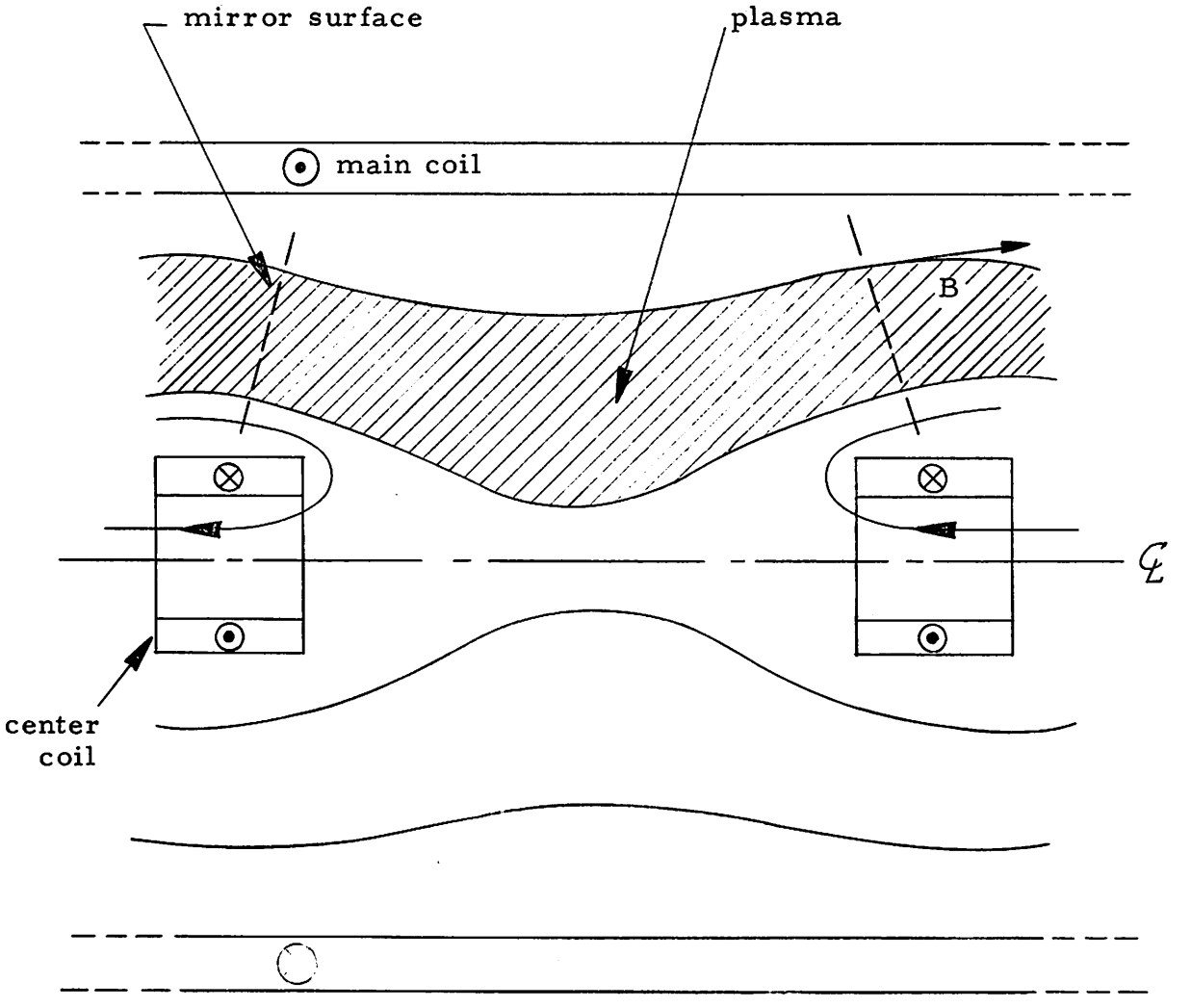

Fig. 6. Hollow plasma configuration.

the plasma boundary. This can be avoided by using an audio frequency electric field whose period of oscillation is much shorter than the transverse relaxation time.

ACKNOWLEDGMENT

We are grateful to C. W. Hartman of UCLRL, Livermore for introducing us to the general idea of studying high temperature plasma instabilities with low temperature plasmas and for use of some of his early calculations. We are also indebted to S. A. Colgate for similar encouragement and fruitful discussions.

REFERENCES

1964 N. Rynn, "Improved Quiescent Plasma Source," Rev. Sci. Inst., Vol. 35, No. 1, pp. 40-46; January.

1957 M. Rosenbluth and C. Longmire, "Stability of plasmas confined by magnetic fields," Ann. Phys., Vol. 1, p. 120, N.Y.

1962 L. Spitzer, Physics of Fully Ionized Gases, Interscience Publishers, Div. of J. Wiley and Sons, 2nd Edition, N.Y.

1961 D. Rose and M. Clark, Plasmas and Controlled Fusion, MIT Press, and J. Wiley and Sons, N.Y.

1962 M. Rosenbluth, N. Krall, N. Rostoker, Nuclear Fusion, Supplement, Part I, p. 143.

1963 R. F. Post, "Observation of plasma instability with rotational effects in a mirror machine," University of California Radiation Laboratory 7302.